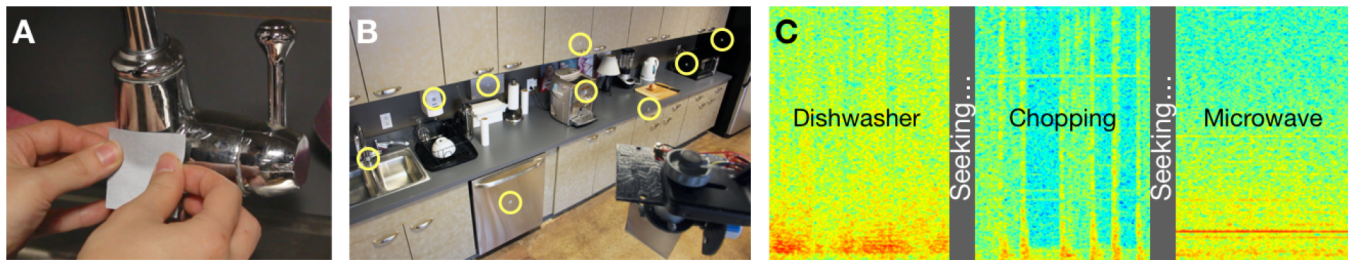# Vibrosight: Long-Range Vibrometry for Smart Environment Sensing

Yang Zhang   **Gierad Laput**   **Chris Harrison**
Human-Computer Interaction Institute, Carnegie Mellon University
5000 Forbes Avenue, Pittsburgh, PA 15213
{yang.zhang, gierad.laput, chris.harrison}@cs.cmu.edu

Figure 1. Users can tag objects (A) they wish to reveal to Vibrosight. The system (B, lower right) periodically scans the room to find retroreflective tags (highlighted with yellow circles), which can be used to sense vibration at long distance. The resulting spectrograms (C) can be used to infer appliance use and human activities.

ABSTRACT

Smart and responsive environments rely on the ability to detect physical events, such as appliance use and human activities. Currently, to sense these types of events, one must either upgrade to "smart" appliances, or attach aftermarket sensors to existing objects. These approaches can be expensive, intrusive and inflexible. In this work, we present Vibrosight, a new approach to sense activities across entire rooms using long-range laser vibrometry. Unlike a microphone, our approach can sense physical vibrations at one specific point, making it robust to interference from other activities and noisy environments. This property enables detection of simultaneous activities, which has proven challenging in prior work. Through a series of evaluations, we show that Vibrosight can offer high accuracies at long range, allowing our sensor to be placed in an inconspicuous location. We also explore a range of additional uses, including data transmission, sensing user input and modes of appliance operation, and detecting human movement and activities on work surfaces.

Author Keywords

Context-Aware Sensing; Internet-of-Things; Appliance Monitoring; Activity Detection; Laser Vibrometry.

INTRODUCTION

Robust activity detection is the foundation for context-aware computing, where systems can not only take commands from users, but also proactively adapt or respond to users' tasks [2, 60]. Today, the closest we have come to achieving this vision commercially is with "smart" appliances (e.g., refrigerators, coffee machines). Another approach that has seen some commercial success are aftermarket "sensor tags" that can be affixed to existing objects to enable some level of smartness (e.g., Notion [37], Motion Cookies [49]). Though direct physical contact yields high signal fidelity, it also limits sensor placement (possibly forcing the use of batteries) and typically means that many sensors must be deployed to monitor an entire room. These sensors can be costly per unit (often tens of dollars), potentially aesthetically obtrusive, need to be water and impact resistant, and require wireless communication infrastructure. We are also beginning to see camera-driven products with activity recognition capabilities (e.g., Matrix Sensor [34], Lighthouse [31]), which have the significant benefit of being able to monitor a wide area without direct instrumentation, though simultaneously suffer from privacy implications, especially in the home.

In this work, we leverage vibrations, which have been shown to be a rich signal source for detecting a wide array of events (see e.g., [28]). Indeed, almost all physical activities generate vibration as a byproduct, whether it be chopping vegetables, writing on a whiteboard, typing on a laptop, running on a treadmill, or even sitting and reading a book. Likewise, many devices and appliances produce characteristic vibrations (e.g., faucets, kitchen appliances, HVAC, power tools, and even electronics if they contain fans). In response, there has been significant prior work leveraging vibrations for activity detection, including sensors coupled to floors and walls [4,

28, 29, 40, 48], as well as plumbing, gas and HVAC infrastructure [6, 9, 14, 17].

In this paper, we describe our work on Vibrosight – a low-cost, vibration sensing approach that works at long distances, affording flexibility in placement. Users affix small, inexpensive, passive stickers (Figure 1A) to objects they wish to reveal to our system – surfaces and objects without tags are invisible to Vibrosight. By using a steerable mirror, we can direct our sensing to any point with line of sight. We use this ability to intensively scan a scene for tags (Figure 1B), and then once found, rapidly cycle between tags to sense the vibrations of their host surfaces. We use this data to produce vibrational spectrograms for each object (Figure 1C), which we feed to a machine learning pipeline for recognition. In our evaluation, we investigated sensing accuracy across 24 objects in four locations. Our system can detect activation at 98.4% accuracy, with a false positive rate of 0.7%. To underscore Vibrosight's robustness to interference, most of our study data were collected with multiple active appliances. Overall, we believe this work illuminates a new sensing approach with unique strengths.

INSPIRATION

We were initially inspired by light-based eavesdropping devices invented by Léon Theremin in the 1950s [18]. These setups bounced light off of distant, large, reflective surfaces – most often windows – and measured the intensity of the reflected light. Vibrations, induced by e.g., voice, cause surfaces to oscillate, which in turn, slightly alters the light path. This manifests as an amplitude modulated signal that can be captured by a photosensor placed in the reflected light. Today, these devices use lasers as their light source and are called "laser microphones".

Unfortunately, traditional setups suffer from two significant drawbacks that preclude their immediate use for activity sensing. First, the method is compatible with very few materials and surfaces. Windows are traditionally used because they are reflective, large and somewhat elastic, and thus function in a similar manner to a microphone diaphragm; airborne sounds, such as speech, cause the glass to oscillate. However, by using a window as a proxy to capture sounds, individual vibrational signals cannot be separated. A second, even greater drawback is that laser microphones are at the mercy of an environment's geometry. Unless the setup can be perfectly perpendicular to e.g., a window, the emitter and receiver must be placed apart in accordance with the reflective angle of incidence. This means sensing multiple surfaces almost certainly means having to deploy multiple sensing setups.

We found that these limitations could be removed by using inexpensive, retroreflective stickers (Figure 1A). These reflect light back to its source, allowing us to combine a laser and photosensor into single, compact sensing unit (Figures 1 and 8). Unlike co-opting a window as a diaphragm, our tags allow us to exclusively read the vibrations of a host surface. This spatial precision makes our technique robust to noisy environments and vibrational interference, and means we can

support recognition of multiple simultaneous activities, which most prior systems do not demonstrate (e.g., [13, 15, 53]).

RELATED WORK

Vibrosight intersects with three key literatures. First, we discuss prior work on human activity detection, focusing on systems that can detect activities from afar, as opposed to sensor tags or wearables. We then discuss prior work that used lasers for sensing and conclude with a review of non-contact vibrometry methods.

Activity Detection

Many approaches have been employed to detect activities. Most popular are camera-based, computer vision systems [27, 31, 34, 44, 68], including depth cameras [54, 66] that ease the task of user segmentation. Researchers have also used thermal sensors, which capture black body radiation from the human body [24, 33]. For a more comprehensive review of this literature, please refer to [7, 25].

There are also many electrical approaches for detecting appliance use. For example, ElectriSense [19] and Dose [8] sense electromagnetic interference (EMI) on powerlines to detect appliances. Wall++ [67] uses painted antennas to capture air-borne EMI signals to detect and localize appliances. Researchers have also attached RFID tags to objects of interest to monitor their usage with remote readers [30, 50, 52]. Finally, it is possible to use radar to recognize objects [5, 63], which could enable context-aware applications.

More relevant to Vibrosight are sensing methods that leverage vibrations to infer activities. The most straightforward approach is to tag objects with sensors that contain accelerometers [37, 49, 56]. To avoid direct instrumentation, researchers have investigated infrastructure mediated approaches, such as attaching vibroacoustic sensors to e.g., gas lines [9] and water pipes [6, 14, 17]. Vibration sensing has also been attempted at building scale [3] for applications including occupancy monitoring [40], tracking [48] and fall detection [4]. Finally, Synthetic Sensors [29] demonstrated hardware featuring many discrete sensors – including a high-speed accelerometer for vibration sensing – that could detect a wide range of activities across an entire room from a single instrumented point.

Lasers for Sensing

Lasers have long been used in sensing systems, including laser tachometers measuring rotary speed and laser velocimeters that measure the speed of surfaces and particles. It is also possible to measure distances with lasers (i.e., LIDAR), either by measuring parallax or phase shift of returned laser light. Some depth cameras, such as the original Microsoft Kinect and Apple iPhone X TrueDepth camera, include a structured-light laser emitter.

In the research domain, Iyer et al. [22] use retroreflective tags and a scanning laser to find phones in a scene and wirelessly charge them (and could be easily extended to work with our approach). Researchers have also used line lasers to track touch input, estimate finger angle on a touchscreen [55], and
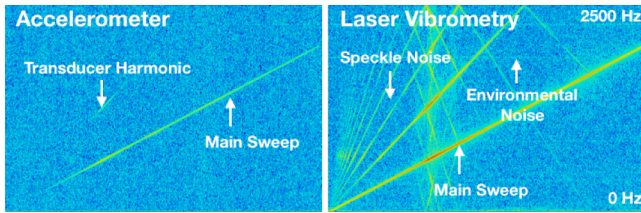
Figure 2. Vibration spectrograms of a swept-frequency signal (0 to 2 kHz) over 20 seconds, measured by an accelerometer (left) and our laser vibrometry sensor (right).

even construct a 3D model of a hand [26]. Reflected laser light produces a unique speckle pattern (one example shown in Figure 3), which researchers have also leveraged. For example, SpecTrans [47] uses the signal to identify objects, SpeckleSense [65] and SpeckleEye [39] track the motion of distant objects, and Smith et al. [51] demonstrate hand gesture recognition.

Non-Contact Vibrometry

Most relevant to our work are non-contact vibrometry techniques, which include RF [57, 61, 62] and high-speed camera approaches [10, 11]. More common is laser vibrometry, which falls into two main categories. The first is laser Doppler vibrometry, which uses the phase difference between reflected, Doppler-shifted light (due to movement of a surface) and an internal reference [23, 36]. There are also intensity-based methods that use high-powered zoom lenses to interrogate laser light falling onto a surface, and sense changes in the speckle pattern resulting from surface vibration [32, 58, 64]. Vibrosight is also intensity-based, but requires no complex optics due to our use of retroreflective tags. Commercial laser vibrometers – used for applications ranging from mechanical analysis to quality control – exclusively rely on laser Doppler vibrometry [38, 42]. Expensive optics mean that even entry-level systems cost tens of thousands of dollars (vs. ~$80 for our Vibrosight prototype). These commercial systems sometimes ship with retroreflective stickers to improve SNR.

BACKGROUND EXPERIMENTS

Although laser vibrometry has been well studied, no previous work has attempted to use it for activity detection in everyday settings. Therefore, prior to the development of our system, we first ran a series of background experiments to verify the principles of operation and investigate parameters that affect sensing quality.

Experiment Apparatus

To generate vibrations of known frequency in our tests, we used a wide-band transducer (driven by an audio amplifier) connected to a signal generator. To measure the photocurrent, we used a PIN photodiode [59] amplified by a standard transimpedance amplification circuit with a 16-2800 Hz bandpass filter. The photodiode was placed next to the laser diode, facing in the same direction. The amplified signal is sampled by an ADC at 5 kHz, which we render into a spectrogram. Of note, all spectrograms in this paper are rendered using a logarithmic color scale.
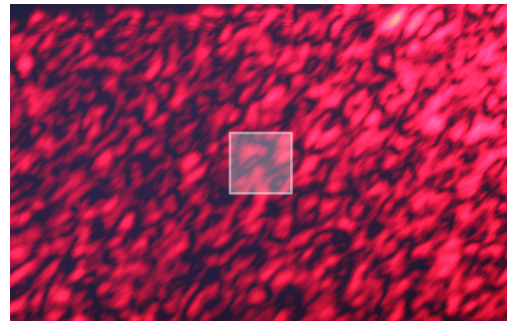

Figure 3. Example retroreflected speckle pattern as captured by a 22×14 mm CMOS sensor at 2 m. A small part of this pattern would land onto the 2.7×2.7 mm photosensor used in Vibrosight (illustrated at scale with white square).

We configured the transducer to output a linear 0 to 2 kHz swept-frequency signal with a peak amplitude of 0.12 G. For reference, a generic microwave we tested had peak vibrational amplitude of 0.45 G. Figure 2, left, shows the vibration signal collected by an accelerometer (STMicroelectronics LIS3DH) affixed to the transducer. Figure 2, right, is data captured using a 3 mW red laser from 5 meters away using a mirror affixed to the transducer. Besides the main sweep, we also see higher-order harmonics (and their aliases) due to the mechanical properties of the transducer and the nature of the reflected laser speckle pattern, specifically the discrete speckles entering and leaving the photosensitive area results in speckle noise [45] (Figure 3). The spectrograms also reveal unwanted environmental noise caused by artificial lighting and electrical noise (Figure 2, right).

Experiment 1 – Laser Wavelength

Laser vibrometry requires a laser beam to illuminate a surface of interest, which naturally leads to the first parameter to investigate: the wavelength of laser light. We tested three common wavelengths: 532 nm (green), 635 nm (red), and 940 nm (infrared) to see if performance varied. As before, we used a 0-2 kHz swept-frequency signal with a mirror attached to our transducer. We placed our laser-photodiode unit 1 m away; see Figure 4 for spectrograms.

The three laser wavelengths had nearly identical performance, though we did notice that the driver circuit of our green laser seemed to be more prone to harmonics of power-line noise. In real-world use, an infrared laser might be preferred, as it is invisible to humans (and eye-safe at the wattage we use). However, for ease of debugging, we selected the red laser for all future experiments.
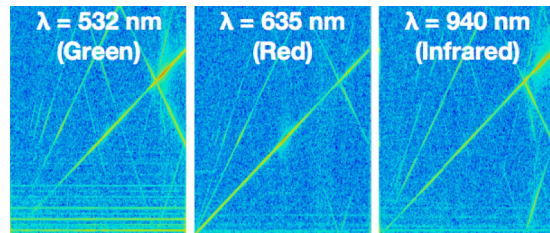
Figure 4. Vibration spectrograms of a swept-frequency signal (0-2 kHz) using lasers of different wavelengths.
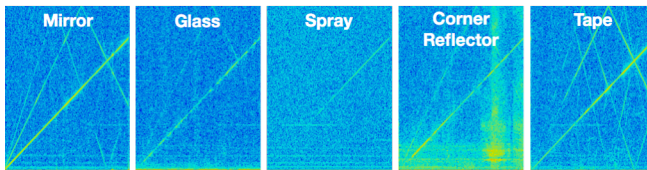
Figure 5. Vibration spectrograms of a swept-frequency signal (0-2 kHz) using different reflective materials.

Figure 7. Vibration spectrograms of a swept-frequency signal (0-2 kHz) under different lighting conditions.

Experiment 2 – Reflective Materials

Our next test was to investigate the performance of different reflective materials. In addition to the previously used mirror, we included (soda-lime) glass and three common retroreflective materials: retroreflective tape [1], retroreflective spray [46] and a (bicycle) corner reflector matrix [12]. We used the same setup and procedure as the previous test. Of note, glass uniquely permits the passage of some laser energy, reflecting approximately 30% (when normal to emitter), which indicates that sensing through glasses could be achieved if desired.

The resulting spectrograms can be seen in Figure 4. The retroreflective spray returned little signal, while the corner reflector generated noise due to physical resonance on the transducer. The mirror, glass, and retroreflective tape all performed well. As noted previously, retroreflective surfaces enable Vibrosight to sense objects at a wide range of angles, and so we adopted retroreflective tape as our tag material of choice.

Experiment 3 – Tag Distance and Angle

Users can tag objects in the environment at any angle and distance, and so we wished to quantify the performance of our selected retroreflective tape with these factors. For this test, we configured the transducer to output a constant 1 kHz vibration and measured the amplitude of the detected signal (at 1 kHz) with the noise floor subtracted. We tested distances from 1 to 8 meters (1 m interval) and angles from 0° to 60° (15° increments).

As seen in Figure 6, the returned signal decreases as distance and angle increases. However, even at 8 meters and 60°, the returned signal is still detectable with our setup (0.04 Vpp). This range of sensing should be sufficient to cover typical
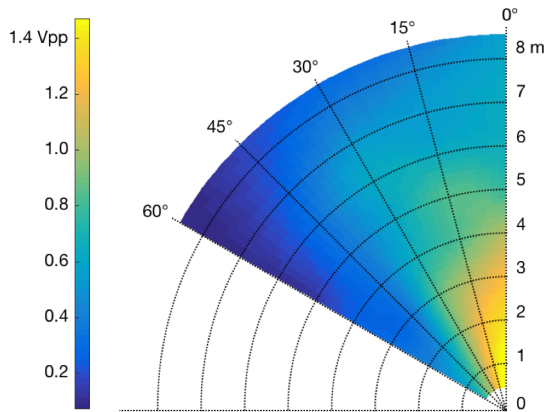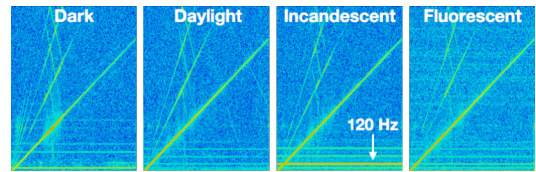
indoor spaces. Longer distances and acuter angles could be enabled with higher-power lasers and superior analog frontends.

Experiment 4 – Artificial and Natural Light

In the previous tests, we found that the most significant source of noise comes from lighting in the environment. In this experiment, we investigated how light – both natural and artificial – affects our approach. We used the same setup as above, at 1 m, using a 0-2 kHz swept-frequency signal. We varied the lighting conditions: dark, daylight, incandescent and fluorescent light.

We found very little difference between dark and daylight conditions, suggesting that natural light level has little effect (Figure 7). This is because our circuit's bandpass filter removes the DC bias of a constant light source. However, artificial light oscillates, which is visible in the captured signal. Additionally, fluorescent lights tend to emit wide-band electrical noise.

Experiment 5 – Speech

During previous tests, we serendipitously noticed our setup was insensitive to voice. As a test, we affixed a tag to a large window, roughly 1×2 m in size, which would be an excellent surface for a conventional laser microphone to capture speech. However, we found that our setup could not detect speech at any volume.

As a more formal test, we recruited four participants (two female) to read aloud a 51-word paragraph, 1 meter away from the window. Using the same setup as the previous experiments, we recorded vibrations while participants spoke. We then played the recordings back to participants, who all reported that they could not hear their voice. Our own analysis suggested there is no discernable signal. As a further test, we affixed an accelerometer to the window, similar to our earlier transducer tests, and recorded vibration during speech. As with our laser vibrometer, we saw no signal, suggesting the magnitude of vibrations induced by speech is very small (under the ~0.001 G noise floor of the accelerometer), and many orders of magnitude lower than vibrations from e.g., motor-driven appliances. That said, it might be possible to recover voice with a more sensitive analog frontend. However, by limiting the signal gain in hardware, we obtain a beneficial privacy-preserving effect.

IMPLEMENTATION

To make our sensor compact and easy-to-deploy, we built a custom sensor board and pan-tilt mirror platform (Figure 8). In total, our prototype hardware cost roughly $80.
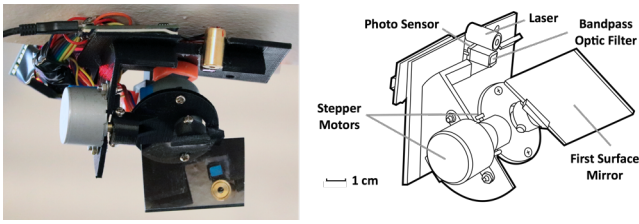

Figure 6. Signal amplitude at different retroreflective tag distances and angles.

Figure 8. Left: Vibrosight deployed on a celling; laser diode and photosensor can be seen in the mirror's reflection. Right: Illustration of key components.

Sensor

Our sensor (Figure 8) consists of two main elements. First is a 3 mW, class IIIA, red laser diode (Quarton VLM-635 [43]), which is rated as safe for brief, direct exposure to the naked eye [21]. In our scanning mirror design, the duty cycle at any one position is low, and as we discuss later, we can detect when the beam is interrupted and turn off the laser as an extra safety measure (similar to [22]). The second component is a 2.7×2.7 mm square PIN photodiode [59] fitted with a 635±18 nm bandpass optical filter. To further reduce the effect of ambient light and improve directionality, we house our photodiode in a 2 cm long, black plastic tube.

Pan-Tilt Mirror Platform

To sense multiple objects in an environment, we designed a mirror-control platform, built from two BYJ-48 stepper motors [35] and a 5×5 cm first surface mirror (Figure 8). This platform has a 120° (pan) by 60° (tilt) field of view with an angular resolution of 0.18°. We run our stepper motors at 30°/sec. To remove gear backlash, our driver software seeks to a point 6° above and to the left of a point, before translating to the desired target.

Driver/Sensor Board

Our driver/sensor board (Figure 9) is built around an MK20DX256VLH7 microcontroller [16] powered by Teensy 3.2 firmware [41]. Eight digital pins are used to control the two stepper motors. The board also features a 16-2800 Hz bandpass analog frontend with a programmable gain. The amplified signal is sampled by the built-in ADC on the microcontroller at 5 kHz. A second analog frontend (no bandpass) measures the absolute reflected light intensity. Data is sent to a laptop over USB for visualization and further computation.

Tags

We used 3M 79961 Scotchlite Reflective Striping Tape [1] for our tags. To ensure Vibrosight can find tags, even at long distances, they cannot be smaller than the step size of our mirror-control platform. The formula to calculate the minimum size of a tag given stepper motor angular resolution and sensor distance is:

$$Tag\ Size \geq 2 \times \sin(Angular\ Resolution/2) \times Distance$$

For example, when sensing at 4 m with our prototype's 0.18° angular step size, the minimum tag size would be 1.3×1.3 cm. At longer sensing distances, larger tags must be used. We selected 5×5 cm as our standard tag size, which
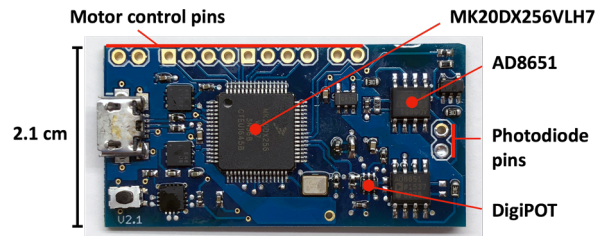

Figure 9. Vibrosight driver/sensor board.

was sufficient for all of our tests and locations. At small-volume retail prices, these tags cost 30 cents each.

Tag Search

To find tags, Vibrosight raster scans its field of view from top to bottom while measuring the absolute reflected light intensity at each step. If the laser hits a tag, the intensity of reflected light significantly increases, manifesting as a peak in our scanned signal. When the raster scan is complete, we spatially cluster all peaks to extract the theta and phi of probable tags. On our prototype hardware, this scanning process takes 20 minutes and is chiefly limited by the speed of our stepper motors. We envision this process being triggered by users when they tag a new object they wish to register with the systems. However, tag search could also occur opportunistically throughout a day, such that new objects are found within a few hours automatically.

Tag Labeling

Our search process finds tags in a scene, but cannot identify what objects they are attached to. One option is for users to provide labels, for example, our system could flash a visible laser onto a tag and ask "what is this?" (e.g., by voice interface or smartphone app). Alternatively, our system could automatically identify objects based on their vibrational signal (e.g., pre-loaded library) when they first run, which we show is possible in our subsequent evaluation.

Signal Processing & Featurization

After our system finds all tags in its field of view, it cycles between them in a round robin fashion. We used a traveling salesman solver to find the shortest path between known tags. While seeking, the laser is turned off. Once a target is reached, our system waits half a second for mechanical oscillations to dampen. The laser then turns on and one second of data is recorded. We compute a spectrogram using a 50% overlapping, 512 window-sized FFT, which we use to compute the max, mean, and standard deviation for each frequency band (256×3 values), resulting in 768 features for machine learning.

Detection

For each object (i.e., tag), we train a two-class classifier: *active* and *inactive*. We used a Random Forest implementation (default parameters) provided by Weka [20]. When Vibrosight seeks to an object, the corresponding classifier is fed live data to detect activity. As each object classifier is independent, we innately support the detection of simultaneous events, and can easily add new object classifiers.
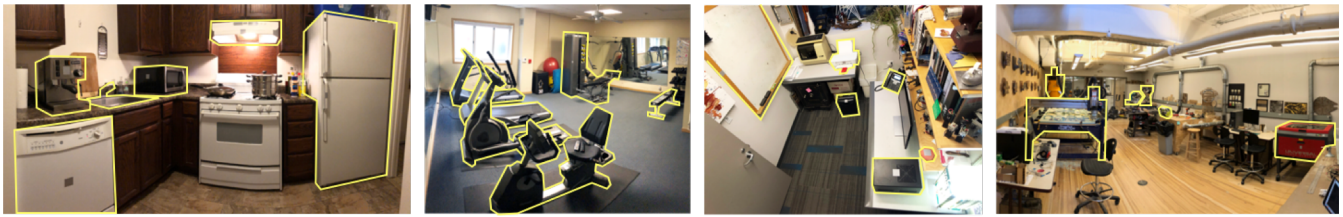
Figure 10. Our 4 test locations and 24 objects (outlined in yellow). From left to right: Kitchen, Gym, Office and Workshop.

Open Source

We make all source files (PCB design, 3D models, embedded firmware, and software) available online for replication: https://github.com/FIGLAB/Vibrosight. We also include all data collected in our evaluation, described in the next section.

EVALUATION

To investigate the accuracy of Vibrosight, we ran a multi-stage evaluation in four indoor contexts: kitchen, gym, office and workshop. For portability, we deployed Vibrosight on a tall tripod, which we placed in the corner of each room. Within each context, we selected six common objects to test (Figure 10), which we tagged with line of sight to our sensor. Active signals from all tested objects can be seen in Figure 11, while Table 1 provides the distances and angles of the tags.

Before collecting vibration data, we first ran three rounds of tag search as a test. We recorded the number of missed tags and any false positive tags found, manually correcting the data before proceeding. In each location, Vibrosight cycled between tags, collecting three seconds of data from each object for four conditions:

No Objects Active – All objects were turned off, with each object tag being sensed ten times in total (for each tag: 10 cycles × 3 seconds of data)
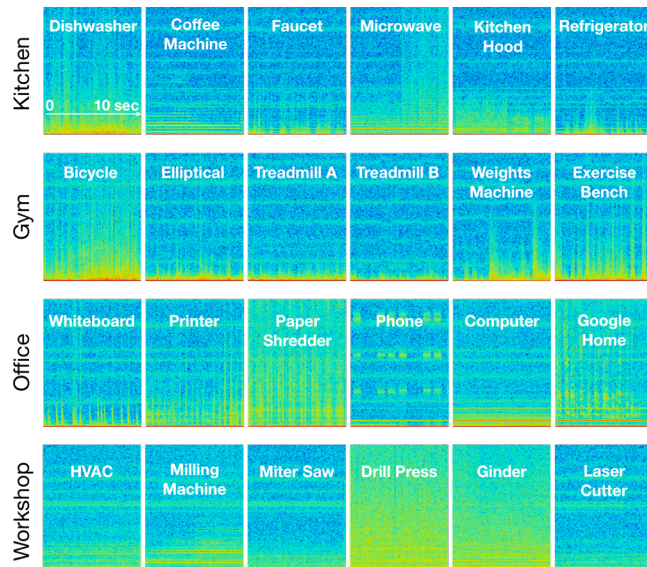

**Figure 11. Vibration spectrograms (0 to 2.5KHz)
of our 24 test objects when active.**

One Object Active – One object at a time was turned on, followed by ten rounds of data collection for all objects (for each tag: 10 cycles × 6 active objects × 3 seconds of data).

Two Objects Active – Two objects at a time were turned on, followed by ten rounds of data collection for each pairwise combination (for each tag: 10 cycles × 15 active object pairings × 3 seconds of data)

All Objects Active – All six objects in the room were turned on simultaneously, with each object being sensed ten times in total (for each tag: 10 cycles × 3 seconds of data)

This procedure yielded 5,040 *active* instances and 11,520 *inactive* instances from our 24 objects.

RESULTS

Tag Search Accuracy

Across the 12 rounds of tag search we performed (4 locations × 3 rounds, with each location containing 6 tagged objects), Vibrosight failed on a single tag twice, resulting in a tag search accuracy of 97.2%. We note that no tags were missed when results from all three passes were combined. There were no false positive tags.

Usage Detection Accuracy

To investigate Vibrosight's ability to detect if an object is active, we ran a leave-one-round-out cross-validation. Specifically, we trained detection classifiers on nine rounds (i.e., seek cycles) of collected data, and tested on the remaining round (all combinations, results averaged). This procedure prevents data with time adjacency from being included in both the train and test dataset.

Across all objects, locations and conditions, Vibrosight achieved an average detection accuracy of 98.4% (SD=1.6). False positive activations are low: 0.7% (SD=0.5). We break out True Positive and False Positive rates across objects in Table 1. We found no correlation in accuracy between tag distance and angle.

Vibrational Interference

Vibrational interference can occur when objects vibrate so strongly that signals propagate through a structure and shake other objects. This can cause false positives, as *inactive* objects can begin to vibrate. Another failure mode occurs when an *active* appliance's vibration signal changes due to the superimposition of an external vibration, resulting in a new (i.e., unlearned) signal that can decrease true positive accuracy.

Location	Object	Distance to Sensor	Tag Angle	True Positive Rate	False Positive Rate
Kitchen	Dishwasher	1.18 m	34 °	98.1 %	0.8 %
	Coffee Machine	1.21 m	29 °	88.1 %	0.4 %
	Faucet	1.84 m	40 °	96.2 %	4.4 %
	Microwave	2.14 m	45 °	98.6 %	1.5 %
	Kitchen Hood	1.92 m	10 °	98.6 %	0.9 %
	Refrigerator	1.56 m	33 °	93.8 %	1.1 %
Gym	Bicycle	1.61 m	12 °	97.6 %	0.2 %
	Elliptical	2.50 m	8 °	100.0 %	0.2 %
	Treadmill A	3.48 m	13 °	99.0 %	0.0 %
	Treadmill B	4.78 m	35 °	99.0 %	0.0 %
	Weights Machine	5.89 m	42 °	99.0 %	0.0 %
	Exercise Bench	4.23 m	28 °	98.6 %	0.4 %
Office	Whiteboard	2.28 m	28 °	97.1 %	0.2 %
	Printer	2.68 m	38 °	97.6 %	0.8 %
	Paper Shredder	2.79 m	10 °	98.1 %	0.2 %
	Phone	2.18 m	18 °	82.4 %	0.2 %
	Computer	1.26 m	39 °	93.3 %	1.5 %
	Google Home	1.28 m	42 °	93.8 %	1.0 %
Workshop	HVAC	7.68 m	8 °	99.5 %	0.0 %
	Milling Machine	4.09 m	14 °	97.6 %	0.4 %
	Miter Saw	8.73 m	28 °	97.1 %	0.8 %
	Drill Press	8.25 m	28 °	98.6 %	0.0 %
	Grinder	5.25 m	32 °	100.0 %	0.0 %
	Laser Cutter	3.44 m	20 °	87.1 %	1.3 %

Table 1. Deployment details and accuracies for the 24 objects.

To understand the effects of vibrational interference on our system, we break out results into the four data collection conditions in Table 2. There was a small, but significant decrease in accuracy (2.3%) from *one object active* (no interference possible) to *two objects active* (potential for interference) conditions (paired t-test; p<.05). The confusion matrices suggest that objects that sat on a common surface (e.g., table) experienced some interference. For example, in our kitchen location, the microwave and coffee machine sat on a common granite countertop, and interference between these two devices was responsible for 33.4% of all detection errors in the kitchen.

Sampling Duration

Shorter sampling durations per object are beneficial, as it allows Vibrosight to cycle between tags in a scene more rapidly, allowing for detection of shorter activations and with less latency. However, less data could also lead to a decrease in detection accuracy.

	True Positive Rate	False Positive Rate
No object active	NA	1.3%
One object active	97.9%	0.5%
Two objects active	95.6%	0.7%
All objects active	97.5%	NA

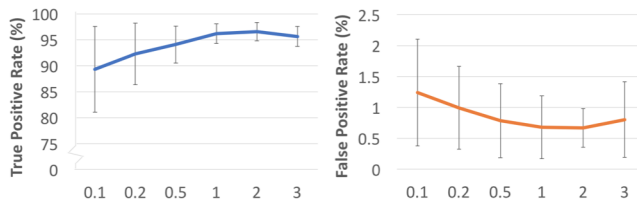**Table 2. Accuracies across data collection conditions.**

Figure 12. Average accuracy vs. sampling duration (seconds).

To investigate this effect in our study, our procedure recorded three seconds of data from each object per seek. In a post hoc experiment, we followed the same validation procedure as above, but varied our train and test data in duration from 0.1 to 3.0 seconds. We used the same 768 machine learning features, which are duration independent. As expected, accuracy drops as sampling duration decreases – Figure 12 plots this result. However, the drop in accuracy is not consistent across devices. Those with intermittent vibrations, such as the phone ringing (which contains pauses of ~1 second) are most impacted, while devices with consistent output (e.g., coffee grinder) are unaffected down to around 0.2 seconds. One second sampling duration appears to be a good tradeoff between speed and accuracy.

Robustness Across Time

To test Vibrosight's performance across time, we ran a second session of data collection separated by one week. We placed our setup in a similar (but not exactly the same) location. The data collection procedure was the same as before, except that we collected five rounds (i.e., seek cycles) of data instead of ten (resulting in 2,520 active and 5,760 inactive instances). We ran this newly collected data through our pretrained classifiers from week one. Average accuracy was 96.2% (SD=2.1), with a false positive rate of 2.3% (SD=2.3), which was not significantly different than week one accuracy, suggesting robustness across time.

Object Identification

So far, we have only discussed Vibrosight's ability to detect if objects are *active* or *inactive*. However, we found that vibrations of different appliances are quite unique (see Figure 11) and might be used to infer object *type* without user labeling. For this test, we evaluated the accuracy of a 24-class object classifier (SMO, Poly Kernel with E=1.0) using a leave-one-round-out cross-validation (week one data, all conditions, active instances only).

Across our 24 objects, average identification accuracy was 92.1% (SD=5.9); the confusion matrix is offered in Figure 13. We can see that most of the confusion occurs within a

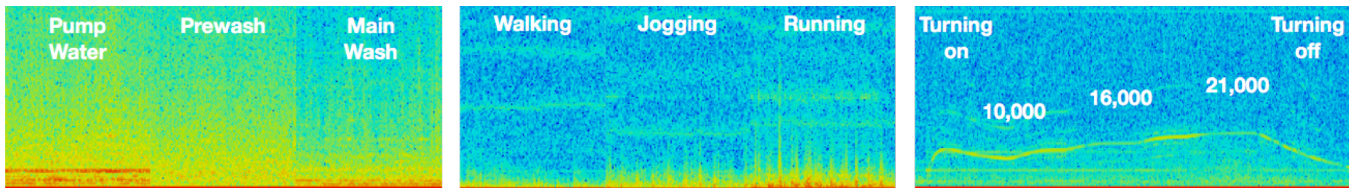**Figure 13. Confusion matrix of object identification (%).**

Figure 14. Vibration spectrograms (0 - 500 Hz) of a dishwasher (left), treadmill (middle), and milling machine (right) in different modes of operation.

location. We suspect this is due to the classifier overfitting to environmental noise (both lighting and EMI) and also vibrational interference between objects, where one object's vibration is being picked up by another. Additionally, in the case of the gym, we included two objects of the same type (treadmill). If we discount confusion between the two treadmills as an error, average object identification accuracy is 92.8% (SD=5.5).

SUPPLEMENTAL STUDIES & APPLICATIONS
We now describe a series of focused, supplemental studies, as well as additional applications enabled by Vibrosight.

Sensing Modes of Operation
We found that many appliances vibrate uniquely when in different modes of operation, especially motor-driven appliances. Figure 14 offers three examples: a dishwasher at different cleaning phases, a treadmill when a user is walking/jogging/running, and a milling machine at different RPMs. Vibrosight can easily leverage these characteristic signals to enable richer, object-specific classifiers.

Detecting Objects and Activities on Work Surfaces
One potential limitation of Vibrosight is that it is ill-suited for tracking small appliances that move around, such as blenders and staplers. We found, however, that we can tag host surfaces to capture vibrations. For example, Figure 15 shows data and detection results from a tagged work surface, on top of which a user hammers, hand files and sweeps. This property allows Vibrosight to detect a much wider range of activities beyond large fixed appliances.

To test this ability more formally, we revisited our four test locations and ran a supplemental study. We affixed a tag to one exemplary surface in each location and developed a new set of test classes: *kitchen countertop* (classes: chopping, coffee grinder running, kettle boiling, blender running), *office table* (classes: typing, writing), *workshop table* (classes: hammering, hand filing, sawing), and *gym mat* (classes: jumping jacks, push-ups). Similar to our main study, we collected 3 seconds of data for each class (including *no activity*)
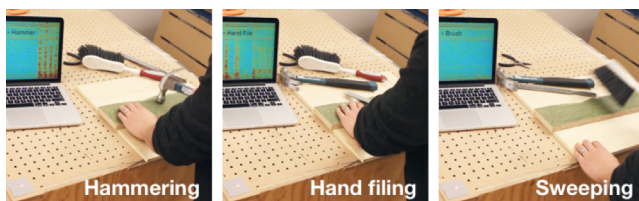

Figure 15. Vibrosight detects activities on a work surface. Signal and classification shown on laptop for illustration.

× 10 rounds. We then ran a leave-one-round-out cross-validation study (per location) using the same featurization and machine learning pipeline as before (i.e., SMO, Poly Kernel with E=1.0). Overall, Vibrosight was able to detect activities using surface vibration data with a mean accuracy of 89.7% (SD=2.3).

Human Movement
Human movement inevitably induces vibrations in the environment. This is especially true for objects such as seating and beds. Figure 16 shows the signal from a sofa as a user sits down, which can be used to detect use and occupancy. Similarly, Vibrosight could monitor sleep restfulness if a tag is placed on a headboard or bedframe.
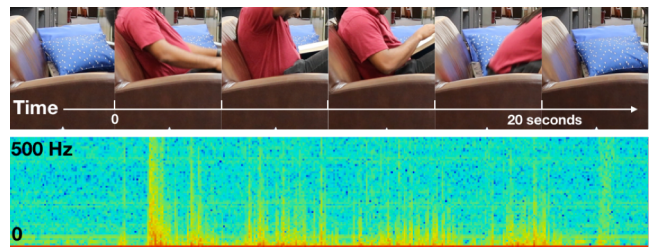
Figure 16. Vibrosight can detect when this couch is in use.

User Input
Vibrations resulting from knocking or tapping on a tagged surface are very apparent to Vibrosight. Thus, it is possible to support basic user input. Figure 17 offers one example where double knocking on a laundry machine instantiates a notification request (as Vibrosight also knows when the laundry machine cycle is complete).

Figure 17. A user double knocks on a laundry machine to request a completion notification.

Data Communication
For devices with speakers, motors or other actuators, it is possible to encode information in the form of vibrations, which can be detected and decoded by Vibrosight. This opens an interesting communication channel for richer applications. For example, devices could emit their brand and model number (allowing a specialized classifier to be loaded), or an IP address to expose additional functionality.

As a proof of concept, we attached a retroreflective tag to the bezel of an LCD TV and used on-off-keying with a 1 kHz carrier emitted through the build-in speakers to broadcast a UID. Figure 18 offers an example transmission, which includes a 6-bit header, 4-bit payload length, 12-bit payload, and 5-bit tail.

Figure 18. Vibrosight can detect encoded vibrations from a TV.

Leveraging Occlusion

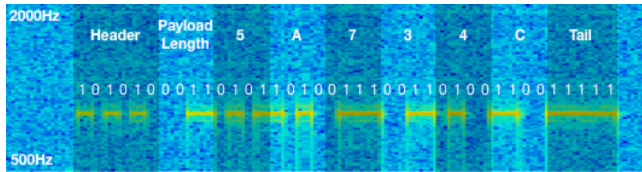Occlusion of tags can also be used to infer activity information. For example, it is possible to strategically attach a tag so that it is occluded when an object is in use, for example, an eyewash station (Figure 19). Occlusion is easily detected by measuring the reflected light intensity.

Figure 19. Tag occlusion is easily detected by measuring the reflected light intensity, and can be used to infer use.

LIMITATIONS

Laser safety was a primary concern from the beginning of the project. To reduce the potential of harm, we limited ourselves to lasers rated Class IIIA or below. It may be possible to use even lower-powered lasers with superior band-pass optics, photodiodes and analog frontend. We also endeavored to reduce the duty cycle as much as possible, not only by scanning, but also with occlusion detection. Specifically, once we seek to a tag and receive no reflected light, we infer the tag is occluded, and immediately turn off the laser (within ~1 ms), limiting accidental exposure.

Similar to other optical approaches, our system requires line of sight and is affected by occlusion. To partially mitigate this, we most often deployed Vibrosight near the ceiling, which affords a good view of rooms. This is also a less conspicuous location and where sensors are typically deployed in commercial settings. If we detect that a tag is occluded, we can simply suspend classification, as opposed to producing an errorful result.

Another limitation is that Vibrosight cannot observe multiple objects simultaneously, as our current implementation reads data from tags in a round-robin manner (pausing at each for e.g., one second). This limits our current system to events with sufficient duration. Fortunately, many appliances and activities have durations on the order of tens of seconds, minutes or even hours. There are also immediate ways to im-

prove our prototype with e.g., faster stepper motors and multiple lasers. Nonetheless, there are transient events (e.g., stapling papers) that can occur and dissipate within ~100 ms, which would likely require a non-time-multiplexed sensing approach.

CONCLUSION

We have presented Vibrosight, a sensing approach for smart environments that uses laser vibrometry. Users can tag objects they wish to reveal to our system, which can then be used to sense vibrations at long distance. Through a series of experiments and evaluations, we demonstrate that our approach robustly detects activities at high accuracies. We also explored a range of supplemental uses for our system. We believe Vibrosight is a new and practical way to enable a wide range of interactive and context-aware applications for smart environment. We hope to encourage future work by open sourcing all project materials.

REFERENCES

1. 3M Inc. Product Datasheet. Retrieved July 16, 2018 from http://multimedia.3m.com/mws/media/305141O/scotchcal-mr-y-accesorios.PDF?fn=1866.PDF

2. Gregory D. Abowd, Anind K. Dey, Peter J. Brown, Nigel Davies, Mark Smith, and Pete Steggles. 1999. Towards a Better Understanding of Context and Context-Awareness. In *Proceedings of the 1st international symposium on Handheld and Ubiquitous Computing* (HUC '99), Springer-Verlag, London, UK, UK, 304-307. DOI: https://doi.org/10.1007/3-540-48157-5_29

3. David E. Allen. Building vibrations from human activities. *Concrete International* 12, no. 6 (1990): 66-73.

4. Majd Alwan, Prabhu Jude Rajendran, Steve Kell, David Mack, Siddharth Dalal, Matt Wolfe, and Robin Felder. A smart and passive floor-vibration based fall detector for elderly. In *Information and Communication Technologies*, 2006. ICTTA'06. 2nd, vol. 1, pp. 1003-1007. IEEE, 2006. DOI: https://doi.org/10.1109/ICTTA.2006.1684511

5. Daniel Avrahami, Mitesh Patel, Yusuke Yamaura, and Sven Kratz. 2018. Below the Surface: Unobtrusive Activity Recognition for Work Surfaces using RF-radar sensing. In *Proceedings of the 23rd International Conference on Intelligent User Interfaces* (IUI '18). ACM, New York, NY, USA, 439-451. DOI: https://doi.org/10.1145/3172944.3172962

6. Tim Campbell, Eric Larson, Gabe Cohn, Jon Froehlich, Ramses Alcaide, and Shwetak N. Patel. 2010. WATTR: a method for self-powered wireless sensing of water activity in the home. In *Proceedings of the 12th ACM international conference on Ubiquitous*

computing (UbiComp '10). ACM, New York, NY, USA, 169-172. DOI: https://doi.org/10.1145/1864349.1864378

7. Jose M. Chaquet, Enrique J. Carmona, and Antonio Fernández-Caballero. A survey of video datasets for human action and activity recognition. *Computer Vision and Image Understanding* 117, 6 (2013): 633-659.

8. Chen, Ke-Yu, Sidhant Gupta, Eric C. Larson, and Shwetak Patel. Dose: Detecting user-driven operating states of electronic devices from a single sensing point. In *Pervasive Computing and Communications* (PerCom), 2015 IEEE International Conference on, pp. 46-54. IEEE, 2015. DOI: https://doi.org/10.1109/PERCOM.2015.7146508

9. Gabe Cohn, Sidhant Gupta, Jon Froehlich, Eric Larson, and Shwetak N. Patel. GasSense: Appliance-level, single-point sensing of gas activity in the home. In *International Conference on Pervasive Computing*, pp. 265-282. Springer, Berlin, Heidelberg, 2010. DOI: https://doi.org/10.1007/978-3-642-12654-3_16

10. Abe Davis, Michael Rubinstein, Neal Wadhwa, Gautham J. Mysore, Frédo Durand, and William T. Freeman. The visual microphone: passive recovery of sound from video. *ACM Trans. Graph*. 33, 4, Article 79 (July 2014), 10 pages. DOI: https://doi.org/10.1145/2601097.2601119

11. Abe Davis, Katherine L. Bouman, Justin G. Chen, Michael Rubinstein, Fredo Durand, and William T. Freeman. Visual vibrometry: Estimating material properties from small motion in video. In *Proceedings of the IEEE Conference on Computer Vision and Pattern Recognition*, pp. 5335-5343. 2015. DOI: https://doi.org/10.1109/TPAMI.2016.2622271

12. Deboc Inc. Product information. Retrieved July 16, 2018 from http://a.co/5nolCSX

13. Eronen, Antti J., Vesa T. Peltonen, Juha T. Tuomi, Anssi P. Klapuri, Seppo Fagerlund, Timo Sorsa, Gaëtan Lorho, and Jyri Huopaniemi. Audio-based context recognition. *IEEE Transactions on Audio, Speech, and Language Processing* 14, no. 1 (2006): 321-329. DOI: https://doi.org/10.1109/TSA.2005.854103

14. James Fogarty, Carolyn Au, and Scott E. Hudson. 2006. Sensing from the basement: a feasibility study of unobtrusive and low-cost home activity recognition. In *Proceedings of the 19th annual ACM symposium on User interface software and technology* (UIST '06). ACM, New York, NY, USA, 91-100. DOI: https://doi.org/10.1145/1166253.1166269

15. Foggia, Pasquale, Nicolai Petkov, Alessia Saggese, Nicola Strisciuglio, and Mario Vento. Reliable detection of audio events in highly noisy environments. *Pattern Recognition Letters* 65 (2015): 22-28. DOI: https://doi.org/10.1016/j.patrec.2015.06.026

16. Freescale Inc. Product Datasheet. Retrieved July 16, 2018 from http://cache.freescale.com/files/32bit/doc/data_sheet/K 20P64M72SF1.pdf

17. Jon E. Froehlich, Eric Larson, Tim Campbell, Conor Haggerty, James Fogarty, and Shwetak N. Patel. 2009. HydroSense: infrastructure-mediated single-point sensing of whole-home water activity. In *Proceedings of the 11th international conference on Ubiquitous computing* (UbiComp '09). ACM, New York, NY, USA, 235-244. DOI: http://dx.doi.org/10.1145/1620545.1620581

18. Albert Glinsky. *Theremin: Ether Music and Espionage*. University of Illinois Press, 2000.

19. Sidhant Gupta, Matthew S. Reynolds, and Shwetak N. Patel. 2010. ElectriSense: single-point sensing using EMI for electrical event detection and classification in the home. In *Proceedings of the 12th ACM international conference on Ubiquitous computing* (UbiComp '10). ACM, New York, NY, USA, 139-148. DOI: https://doi.org/10.1145/1864349.1864375

20. Mark Hall, Eibe Frank, Geoffrey Holmes, Bernhard Pfahringer, Peter Reutemann, and Ian H. Witten. 2009. The WEKA data mining software: an update. *ACM SIGKDD Explorations Newsletter*. 11, 1. 10-18. http://doi.org/10.1145/1656274.1656278

21. Roy Henderson, and Karl Schulmeister. *Laser Safety*. CRC Press, 2003.

22. Vikram Iyer, Elyas Bayati, Rajalakshmi Nandakumar, Arka Majumdar, and Shyamnath Gollakota. 2018. Charging a Smartphone Across a Room Using Lasers. In *Proceedings of ACM Interact. Mob. Wearable Ubiquitous Technol*. 1, 4, Article 143 (January 2018), 21 pages. DOI: https://doi.org/10.1145/3161163

23. Martin Johansmann, Georg Siegmund, and Mario Pineda. Targeting the limits of laser Doppler vibrometry. In *Proceedings of IDEMA* (2005): 1-12.

24. Dharmendra Chandrashekar Kallur. *Human Localization and activity recognition using distributed motion sensors*. Ph.D Dissertation. Oklahoma State University, 2014.

25. Shian-Ru Ke, Hoang Le Uyen Thuc, Yong-Jin Lee, Jenq-Neng Hwang, Jang-Hee Yoo, and Kyoung-Ho Choi. A review on video-based human activity recognition. *Computers* 2, no. 2 (2013): 88-131. DOI: https://doi.org/10.3390/computers2020088

26. David Kim, Otmar Hilliges, Shahram Izadi, Alex D. Butler, Jiawen Chen, Iason Oikonomidis, and Patrick Olivier. 2012. Digits: freehand 3D interactions anywhere using a wrist-worn gloveless sensor. In *Proceedings of the 25th annual ACM symposium on User interface software and technology* (UIST '12). ACM, New York, NY, USA, 167-176. DOI: https://doi.org/10.1145/2380116.2380139

27. Gierad Laput, Walter S. Lasecki, Jason Wiese, Robert Xiao, Jeffrey P. Bigham, and Chris Harrison. 2015. Zensors: Adaptive, Rapidly Deployable, Human-Intelligent Sensor Feeds. In *Proceedings of the 33rd Annual ACM Conference on Human Factors in Computing Systems* (CHI '15). ACM, New York, NY, USA, 1935-1944. DOI: https://doi.org/10.1145/2702123.2702416

28. Gierad Laput, Robert Xiao, and Chris Harrison. 2016. ViBand: High-Fidelity Bio-Acoustic Sensing Using Commodity Smartwatch Accelerometers. In *Proceedings of the 29th Annual Symposium on User Interface Software and Technology* (UIST '16). ACM, New York, NY, USA, 321-333. DOI: https://doi.org/10.1145/2984511.2984582

29. Gierad Laput, Yang Zhang, and Chris Harrison. 2017. Synthetic Sensors: Towards General-Purpose Sensing. In *Proceedings of the 2017 CHI Conference on Human Factors in Computing Systems* (CHI '17). ACM, New York, NY, USA, 3986-3999. DOI: https://doi.org/10.1145/3025453.3025773

30. Hanchuan Li, Can Ye, and Alanson P. Sample. 2015. IDSense: A Human Object Interaction Detection System Based on Passive UHF RFID. In *Proceedings of the 33rd Annual ACM Conference on Human Factors in Computing Systems* (CHI '15). ACM, New York, NY, USA, 2555-2564. DOI: https://doi.org/10.1145/2702123.2702178

31. Lighthouse AI Inc. Product Information. Retrieved July 16, 2018 from https://www.light.house

32. Peter Martin, and Steve Rothberg. Laser vibrometry and the secret life of speckle patterns. In *8th International Conference on Vibration Measurements by Laser Techniques: Advances and Applications*, vol. 7098, p. 709812. International Society for Optics and Photonics, 2008. DOI: https://doi.org/10.1117/12.803156

33. Shota Mashiyama, Jihoon Hong, and Tomoaki Ohtsuki. Activity recognition using low resolution infrared array sensor. In Communications (ICC), 2015 *IEEE International Conference on Communications* (ICC), pp. 495-500. IEEE, 2015. DOI: https://doi.org/10.1109/ICC.2015.7248370

34. Matrix Inc. Product Information. Retrieved July 16, 2018 from http://www.matrix.one

35. MikroElektronika Inc. Product Datasheet. Retrieved July 16, 2018 from https://download.mikroe.com/documents/datasheets/step-motor-5v-28byj48-datasheet.pdf

36. Hani H. Nassif, Mayrai Gindy, and Joe Davis. Comparison of laser Doppler vibrometer with contact sensors for monitoring bridge deflection and vibration. *Ndt & E International* 38, no. 3 (2005): 213-218. DOI: https://doi.org/10.1016/j.ndteint.2004.06.012

37. Notion. Product Information. Retrieved July 16, 2018 from http://getnotion.com

38. Onosokki, Inc. Product Information. https://www.ono-sokki.co.jp/English/hp_e/products/kei-soku/s_v/lv1800.html

39. Alex Olwal, Andrew Bardagjy, Jan Zizka, and Ramesh Raskar. 2012. SpeckleEye: gestural interaction for embedded electronics in ubiquitous computing. In *CHI '12 Extended Abstracts on Human Factors in Computing Systems* (CHI EA '12). ACM, New York, NY, USA, 2237-2242. DOI: https://doi.org/10.1145/2212776.2223782

40. Shijia Pan, Amelie Bonde, Jie Jing, Lin Zhang, Pei Zhang, and Hae Young Noh. Boes: building occupancy estimation system using sparse ambient vibration monitoring. In *Sensors and Smart Structures Technologies for Civil, Mechanical, and Aerospace Systems* 2014, vol. 9061, p. 90611O. International Society for Optics and Photonics, 2014. DOI: https://doi.org/10.1117/12.2046510

41. PJRC Inc. Product Information. Retrieved July 16, 2018 from https://www.pjrc.com/teensy/teensy32.html

42. Polytec Inc. Product Information. Retrieved July 16, 2018 from https://www.polytec.com/us/vibrometry/products/single-point-vibrometers/ivs-500-industrial-vibration-sensor/

43. Quarton Inc. Product Information. Retrieved July 16, 2018 from https://infiniter.com/vlm-635-27-lpt-10-industrial-use-line-laser-wavelength-635-nm/

44. Marcus Rohrbach, Sikandar Amin, Mykhaylo Andriluka, and Bernt Schiele. A database for fine grained activity detection of cooking activities. In *Computer Vision and Pattern Recognition* (CVPR), 2012 IEEE Conference on, pp. 1194-1201. IEEE, 2012. DOI: https://doi.org/10.1109/CVPR.2012.6247801

45. Steve J. Rothberg and Benjamin J. Halkon. Laser vibrometry meets laser speckle. In *6th International Conference on Vibration Measurements by Laser Techniques: Advances and Applications*, vol. 5503, pp. 280-292. International Society for Optics and Photonics, 2004. DOI: https://doi.org/10.1117/12.579760

46. Rust-Oleum Corp. Product Datasheet. Retrieved July 16, 2018 from https://www.rustoleum.com/MSDS/ENGLISH/214944.pdf

47. Munehiko Sato, Shigeo Yoshida, Alex Olwal, Boxin Shi, Atsushi Hiyama, Tomohiro Tanikawa, Michitaka Hirose, and Ramesh Raskar. 2015. SpecTrans: Versatile Material Classification for Interaction with Textureless, Specular and Transparent Surfaces. In *Proceedings of the 33rd Annual ACM Conference on Human Factors in Computing Systems* (CHI '15). ACM, New York, NY, USA, 2191-2200. DOI: https://doi.org/10.1145/2702123.2702169

48. Javier Schloemann, VVN Sriram Malladi, Americo G. Woolard, Joseph M. Hamilton, R. Michael Buehrer, and Pablo A. Tarazaga. Vibration event localization in

an instrumented building. In *Experimental Techniques, Rotating Machinery, and Acoustics*, Volume 8, pp. 265-271. Springer, Cham, 2015. DOI: https://doi.org/10.1007/978-3-319-15236-3_24

49. Sen.se Inc. Product Information. Retrieved July 16, 2018 from https://sen.se/store/cookie/

50. Joshua R. Smith, Kenneth P. Fishkin, Bing Jiang, Alexander Mamishev, Matthai Philipose, Adam D. Rea, Sumit Roy, and Kishore Sundara-Rajan. RFID-based techniques for human-activity detection. *Communications of the ACM* 48, no. 9 (2005): 39-44. DOI: https://doi.org/10.1145/1081992.1082018

51. Brandon M. Smith, Pratham Desai, Vishal Agarwal, and Mohit Gupta. CoLux: multi-object 3D micro-motion analysis using speckle imaging. *ACM Transactions on Graphics* (TOG) 36, no. 4 (2017): 34. DOI: https://doi.org/10.1145/3072959.3073607

52. Andrew Spielberg, Alanson Sample, Scott E. Hudson, Jennifer Mankoff, and James McCann. 2016. RapID: A Framework for Fabricating Low-Latency Interactive Objects with RFID Tags. In *Proceedings of the 2016 CHI Conference on Human Factors in Computing Systems* (CHI '16). ACM, New York, NY, USA, 5897-5908. DOI: https://doi.org/10.1145/2858036.2858243

53. Johannes A. Stork, Luciano Spinello, Jens Silva, and Kai O. Arras. Audio-based human activity recognition using non-markovian ensemble voting. In *RO-MAN*, 2012 IEEE, pp. 509-514. IEEE, 2012. DOI: https://doi.org/10.1109/ROMAN.2012.6343802

54. Jaeyong Sung, Colin Ponce, Bart Selman, and Ashutosh Saxena. Unstructured human activity detection from rgbd images. In *Robotics and Automation* (ICRA), 2012 IEEE International Conference on, pp. 842-849. IEEE, 2012. DOI: https://doi.org/10.1109/ICRA.2012.6224591

55. Yoshiki Takeoka, Takashi Miyaki, and Jun Rekimoto. 2010. Z-touch: an infrastructure for 3d gesture interaction in the proximity of tabletop surfaces. In *ACM International Conference on Interactive Tabletops and Surfaces* (ITS '10). ACM, New York, NY, USA, 91-94. DOI: https://doi.org/10.1145/1936652.1936668

56. Texas Instruments Inc. Product Information. Retrieved July 16, 2018 from http://ti.com/ww/en/wireless_connectivity/sensortag/

57. K. A. Tsolis, and C. J. Baker. Radar Vibrometry: Investigating the Potential of RF microwaves to measure vibrations.

58. A. A. Veber, A. Lyashedko, E. Sholokhov, A. Trikshev, A. Kurkov, Y. Pyrkov, A. E. Veber, V. Seregin, and V. Tsvetkov. Laser vibrometry based on analysis of the speckle pattern from a remote object. *Applied Physics B: Lasers and Optics* 105, no. 3 (2011): 613-617 DOI: https://doi.org/10.1007/s00340-011-4585-1

59. Vishay Inc. Product Information. Retrieved July 16, 2018 from https://vishay.com/docs/81521/bpw34.pdf

60. Mark Weiser. The Computer for the 21st Century. *Scientific American* 265, no. 3 (1991): 94-105. DOI: https://doi.org/10.1145/329124.329126

61. Yan Yan, Louis Cattafesta, Changzhi Li, and Jenshan Lin. Analysis of detection methods of RF vibrometer for complex motion measurement. *IEEE Transactions on Microwave Theory and Techniques* 59, no. 12 (2011): 3556-3566. DOI: https://doi.org/10.1109/TMTT.2011.2172624

62. Lei Yang, Yao Li, Qiongzheng Lin, Huanyu Jia, Xiang-Yang Li, and Yunhao Liu. Tagbeat: Sensing Mechanical Vibration Period with COTS RFID Systems. *IEEE/ACM Transactions on Networking* 25, no. 6 (2017): 3823-3835. DOI: https://doi.org/10.1109/TNET.2017.2769138

63. Hui-Shyong Yeo, Gergely Flamich, Patrick Schrempf, David Harris-Birtill, and Aaron Quigley. 2016. RadarCat: Radar Categorization for Input & Interaction. In *Proceedings of the 29th Annual Symposium on User Interface Software and Technology* (UIST '16). 833-841. DOI: https://doi.org/10.1145/2984511.2984515

64. Zeev Zalevsky, Yevgeny Beiderman, Israel Margalit, Shimshon Gingold, Mina Teicher, Vicente Mico, and Javier Garcia. Simultaneous remote extraction of multiple speech sources and heart beats from secondary speckles pattern. *Optics Express* 17, no. 24 (2009): 21566-21580. DOI: https://doi.org/10.1364/OE.17.021566

65. Jan Zizka, Alex Olwal, and Ramesh Raskar. 2011. SpeckleSense: fast, precise, low-cost and compact motion sensing using laser speckle. In *Proceedings of the 24th annual ACM symposium on User interface software and technology* (UIST '11). 489-498. DOI: https://doi.org/10.1145/2047196.2047261

66. Chenyang Zhang, and Yingli Tian. RGB-D camera-based daily living activity recognition. Journal of Computer Vision and Image Processing 2, no. 4 (2012): 12.

67. Yang Zhang, Chouchang Yang, Scott E. Hudson, Chris Harrison and Alanson Sample. 2018. Wall++: Room-Scale Interactive and Context-Aware Sensing. In *Proceedings of the 2018 CHI Conference on Human Factors in Computing Systems* (CHI '18). ACM, New York, NY, USA, Paper 273, 15 pages. DOI: https://doi.org/10.1145/3173574.3173847

68. Zhongna Zhou, Xi Chen, Yu-Chia Chung, Zhihai He, Tony X. Han, and James M. Keller. Activity analysis, summarization, and visualization for indoor human activity monitoring. *IEEE Transactions on Circuits and Systems for Video Technology*. 18, 11 (2008): 1489-1498. DOI: https://doi.org/10.1109/TCSVT.2008.2005612